

Modeling seasonal variations of ocean and sea ice circulation in the Beaufort and Chukchi Seas: A model-data fusion study

Wang Jia¹, Kohei Mizobata², Hu Haoguo³, Jin Meibing⁴, Zhang Sheng⁴, Walter Johnson⁵, Koji Shimada² and Moto Ikeda⁶

1 NOAA Great Lakes Environmental Research Laboratory (GLERL), 4840 S State Road, Ann Arbor, MI 48108 USA

2 Department of Ocean Sciences, Tokyo University of Marine Science and Technology, 4-5-7 Kounan, Minato-ku, Tokyo, 108-8477, Japan

3 Cooperative Institute for Limnology and Ecosystems Research (CILER), School of Natural Resources and Environment, University of Michigan, 4840 S State Road, Ann Arbor, MI 48108 USA

4 International Arctic Research Center, University of Alaska Fairbanks, Fairbanks, AK 99775-7340, USA

5 Minerals Management Service, Department of Interior, 381 Elden Street, Herndon, VA 20170-4817 USA

6 Graduate School of Earth and Environmental Science, Hokkaido University, Sapporo, Hokkaido, Japan

Received September 20, 2008

Abstract A 3.8-km Coupled Ice-Ocean Model (CIOM) was implemented to successfully reproduce many observed phenomena in the Beaufort and Chukchi seas, including the Bering-inflow-originated coastal current that splits into three branches: Alaska Coastal Water (ACW), Central Channel, and Herald Valley branches. Other modeled phenomena include the Beaufort Slope Current (BSC), the Beaufort Gyre, the East Siberian Current (ESC), mesoscale eddies, seasonal landfast ice, sea ice ridging, shear, and deformation. Many of these downscaling processes can only be captured by using a high-resolution CIOM, nested in a global climate model. The seasonal cycles for sea ice concentration, thickness, velocity, and other variables are well reproduced with solid validation by satellite measurements. The seasonal cycles for upper ocean dynamics and thermodynamics are also well reproduced, which include the formation of the cold saline layer due to the injection of salt during sea ice formation, the BSC, and the subsurface upwelling in winter that brings up warm, even more saline Atlantic Water along the shelfbreak and shelf along the Beaufort coast.

Key words ocean and sea ice circulation, Beaufort and Chukchi Seas, model-data fusion.

1 Introduction

The Beaufort and Chukchi seas (Fig. 1) are an important region where North Pacific water via the Bering Strait encounters the Western Arctic water with seasonal ice in the Chukchi Sea, and both seasonal and perennial ice in the Beaufort Sea. The Chukchi Sea is

mainly featured by the continental shelf, while the Beaufort Sea is characterized by a relatively narrow continental shelf and a deep basin with a narrow, steep shelf slope. More importantly, the Beaufort Sea also features continuous landfast ice along the Alaska Arctic coast, parallel to the 20-m isobath^[1]. In comparison, the landfast ice along the western Alaska coast in the Chukchi Sea is discontinuous. All these features have challenged both observationalists and modelers.

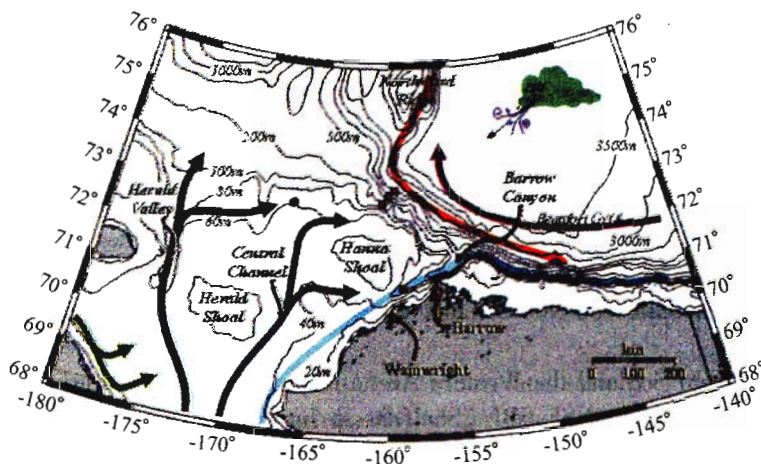


Fig. 1 Schematic diagram for coastal circulation in the Chukchi-Beaufort Seas (light blue: Alaskan Coast Current with the origin of freshwater; Courtesy of Tom Weingartner).

The ocean circulation system in the Beaufort and Chukchi seas is very complex and consists of the Bering inflow that separates into three branches: ACW, Central Channel and Herald Valley branches (see Fig. 1). There are the anticyclonic Beaufort Gyre, the Beaufort Slope Current (BSC), and the East Siberian Current (ESC). The BSC has a spatial scale of about several dozen kilometers^[2,3], and Barrow Canyon Current has a similar spatial scale of about 30 km (Shimada, personal commun.). Another important feature in the Beaufort Sea is the small-scale mesoscale eddies of several dozen kilometers in diameter^[4-6], with anticyclones outnumbering the cyclones. Again, these small-scale features challenge both observation and modeling capability. Particularly, coarse resolution observation arrays and model meshes cannot resolve these processes.

In the shallow Chukchi Sea, tidal current and its mixing should be important^[7,8]. The wind-derived surface waves are also important mechanical sources to vertical mixing. These dynamic sources should be seriously taken into account in both observational and modeling studies.

The winter atmospheric wind pattern is mainly controlled by the anticyclonic (clockwise) Beaufort High, while the summer wind stress is relatively weak due to the weakened Beaufort High. The northward propagating summer storms occasionally move to the Chukchi Sea via the Bering Strait, producing strong wind and mixing. The winter anticyclonic wind stress associated with the Beaufort High has many important effects, such as 1) surface Ekman drift that advects the Beaufort coastal freshwater into the Beaufort Gyre^[9], 2) sub-surface upwelling that brings the warm, saline Arctic intermediate water (i.e., the Atlantic Water) into the Beaufort Sea shelf break, melting surface sea ice^[10], and 3) formation of

landfast ice^[11,12].

An ocean-only model for the Bering-Chukchi shelves was developed during the ISHTAR (Inner Shelf Transfer and Recycling in the Bering-Chukchi Seas) Program by Nihoul *et al.* (1993)^[7]. Though the ISHTAR model included both tidal and wind forcing, the deep basin was excluded (i. e. , the Alaskan Stream, Bering Slope Current, Alaskan Coastal Current, and Kamchatka Current were excluded). Thus the heat and freshwater fluxes were neglected, leaving much to understand concerning this ocean system. Because Nihoul *et al.* 1993 used an ocean-only model, the simulation was conducted only in the ice-free seasons (spring-summer)^[7]. There is no seasonal cycle simulation available for a realistic study of biological cycling. A biological-physical model was also developed, based on Nihoul's ocean model, by Shuert and Walsh (1993)^[13]. The model had the same domain as Nihoul's model, but was confined to the northern Bering Sea and southern Chukchi Sea shelves, again without ice. The shelf break processes and the exchange between the deep basin and continental slope were also ignored as well as other important processes, such as upwelling and mesoscale eddies. The full seasonal cycle of the ecosystem has not yet been simulated.

In the Chukchi Sea and the Western Arctic Ocean, extensive interdisciplinary surveys were conducted under the NSF SBI (Shelf-Basin Interactions) project in the last several years^[14]. These datasets are available for model-data comparison.

Idealized ocean only modeling was conducted by Winsor and Chapman (2004) to study mechanisms of how wind stress affects the Chukchi Sea current system^[15]. An early study by Rutgers University, supported by MMS, also used an ocean only model to simulate ocean circulation in the Beaufort and Chukchi seas. Due to coarse resolution models and other factors, many of the phenomena mentioned above were not resolved.

Our goal is to build a state-of-the-art, stand-alone coupled ice-ocean model to help understand ocean and ice circulation and their dynamic and thermodynamic characteristics in a high-resolution setting. Available measurements will be used to conduct a basic model-data fusion study.

2 Model Description and atmospheric forcing

The CIOM should refer to the studies of Yao *et al.* (2000)^[16] and Wang *et al.* (2002a, b; 2003a, b; 2004, 2005)^[17-22]. The ocean model used is the Princeton Ocean Model (POM)^[23], and the ice model used is a full thermodynamic and dynamics model (Hibler 1980)^[24] that prognostically simulates sea-ice thickness, sea ice concentration (SIC), ice edge, ice velocity, and heat and salt flux through sea ice into the ocean. The model has been successfully applied to the Bering Sea^[25,26], the Beaufort Sea^[27], and in the northern China seas (Q. Liu, personal comm.).

Ocean Model:

- horizontal spherical grid with 3.8 km resolution in longitude and latitude covering the Chukchi-Beaufort seas;
- 24 sigma levels in the vertical;
- open boundaries (velocity, T, and S) are embedded by a climate (atmosphere-ice-ocean-land) GCM from Japan with a resolution of about 25 km with volume transport con-

servation principle and radiation property [28].

- river runoff is applied at the mouth of the Mackenzie River^[29];
- inclusion of parameterization of wind-wave mechanic mixing;
- atmospheric forcing uses National Centers for Environmental Prediction (NCEP)

Reanalysis products; heat flux, mass (moisture) flux, and six-hourly wind stress.

Ice Model:

- full thermodynamics with 2-layer ice and 1-layer snow;
- full dynamics with plastic-viscous rheology under the NCEP forcing^[24,30,31];
- multi-category ice mode^[16,32] fully coupled to an ocean model^[33,34];
- prognostic and diagnostic variables: Ice velocity, compactness, ice edge, thickness, heat budget, salt budget, ice stress, etc.

In this study, ten ice categories (0, 0.2, 0.5, 1, 1.5, 2, 3, 4, 5, and 6 m) are used, each having a percentage in a grid point. Thus, a thickness equation for each category is calculated. Then, the summation of each category thickness is the total thickness at each grid. Thus, sea ice concentration and thickness at each grid are calculated from the sum of the ten ice categories.

The model was spun up with the PHC temperature and salinity^[35], sea ice climatology, January concentration, and motionless sea ice and ocean for the first four years under NCEP reanalysis monthly atmospheric forcing, which were derived from 1958 to 1997. At the bottom layer, both temperature and salinity are restored to the monthly climatology with the same time scale of 60 days. At the surface, salinity, with freshwater flux forcing from P-E, is restored to the observed monthly salinity fields at a time scale of 30 days for prescribing freshwater runoff into the Arctic Basin using the flux correction method of Wang *et al.* (2001)^[28]. After a four-year spinup, a dynamic and thermodynamic seasonal cycle is established. Then, we re-ran the model for another four years using the fourth year output as the restart or initial conditions. During the four-year run, all the monthly atmospheric forcings remain the same. Then, the last year variables are used for examining the seasonal cycle in this study.

3 Model simulations

3.1 General ocean circulation pattern vs. *in situ* observations

The high resolution CIOM reproduced very fine structure of the Alaskan Coastal Current system (three branches) and the anticyclonic large-scale Beaufort Gyre superimposed by mesoscale eddies with anticyclones outnumbering cyclones (Fig. 2). The first branch is the Alaska Coastal Water branch along the Alaska Arctic coast. This current flows mainly along the isobaths with relatively warm water, hugging to the Alaska coast. The second branch (middle) flows northward along the Central Channel and turns to the east, joining ACW/C. The ACW flows eastward all the way to the Canadian Beaufort Sea, encountering the Mackenzie River outflow, where the coastal current then turns sharply to the west and joins the Beaufort Gyre (westward) circulation. As a consequence, between the Beaufort Gyre and ACW current there is a strong horizontal shear, resulting in a deep trough in sea surface height (SSH). This phenomenon is found for the first time using this high resolu-

tion CIOM, and needs field measurements to confirm its existence. The third branch flows northwestward into the Chukchi Sea via a deep channel between the Wrangel Island and Herald Shoal. Part of this current turns to the east and joins the BSC [3]. In addition, the ESC is also reproduced. These features are consistent with recent observations in the region [36].

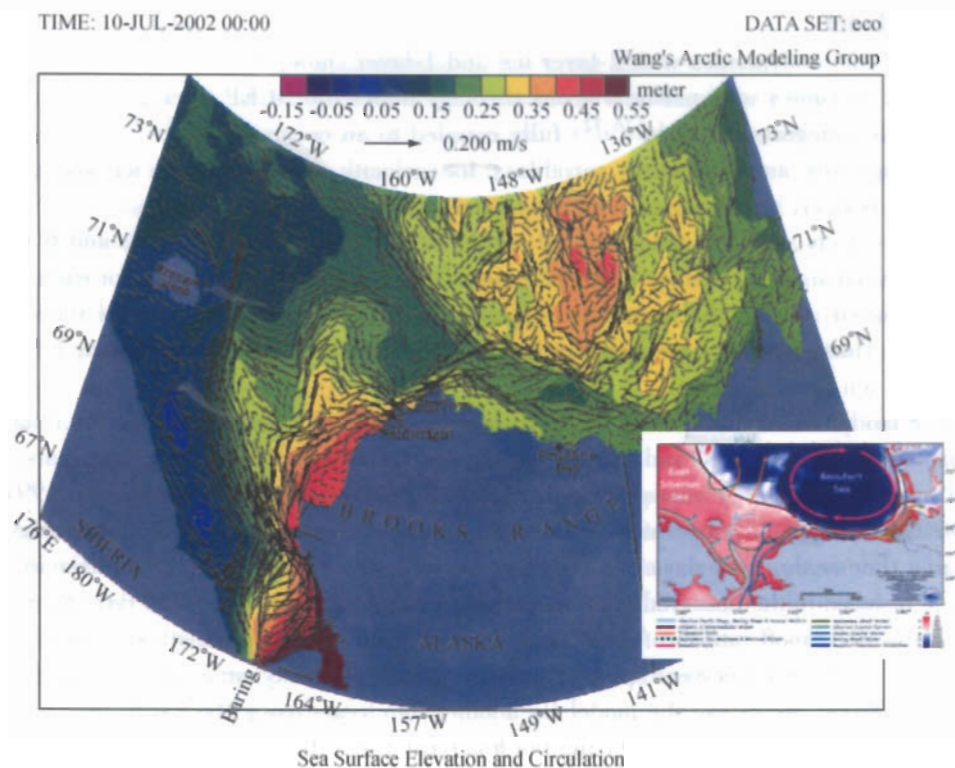


Fig. 2 Model-simulated upmost 50-m averaged ocean velocity on July 10 under climatological forcing, compared with the schematic ocean circulation pattern (imbedded on the lower right corner; courtesy of Weingartner). In the left panel, the color bar indicates the sea level height (SSH) with red being high SSH, while in the right panel, the color bar denotes the bottom topography in meters with red being shallow water.

The simulated Beaufort Gyre is confirmed by the high SSH (red) with anticyclones dominating due to baroclinic instability [6,37]. However, it is not well known whether or not the barotropic instability play a role in triggering mesoscale eddies. Thus, barotropic instability also deserves further investigation.

Both in-situ and satellite remote sensed data are used to validate the Beaufort Sea CIOM. Figure 3 shows the comparison between the model simulation velocity (black) and the ADCP mooring velocity (red) at a subsurface layer of 70 m. The ADCP data were taken from 1992 to 2001 by JAMSTEC (Japan Agency for Marine – earth Science and TEchnology). The simulated velocities are, in general, consistent with the observed. Nevertheless, there are discrepancies in both direction and magnitude, which may be due to the following facts: 1) the model topography/depth was smoothed, 2) the model vertical and horizontal resolution is still coarse, and 3) the model forcing is climatological monthly forcing, while

the observations were taken from 1992 to 2001 by JAMSTEC. Therefore, simulations from year to year (such as from 1990 to present) under the daily forcing are necessary to objectively evaluate the model simulation skills.

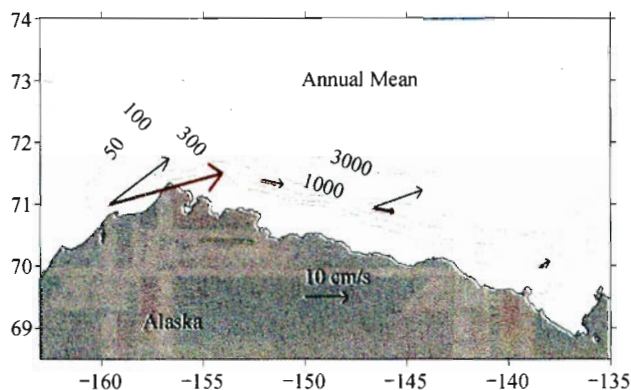


Fig. 3 Climatological annual mean velocity reproduced by the model (black arrows) are compared to the JAMSTEC ADCP-measured velocity (red arrows) at the 70 m depth in the Beaufort and Chukchi seas.

We further validate the CIOM using historical transitional CTD measurements. There were several observational campaigns in the region by JAMSTEC, NSF's SBI (Shelf-Basin Interactions in the Western Arctic) project^[3], Canadian Beaufort Sea project^[10], and MMS-sponsored Beaufort Sea oceanographic survey. Comparisons were conducted using these available data.

Figure 4 shows a transect comparison off Barrow Canyon in the Chukchi Sea. The summer observations show that there is a very saline, thick subsurface layer (see the inserted map at the lower right corner), thought to be the winter dense water that can survive summer. Our model-simulated the monthly salinity maps show that in summer (see August and September maps), the thick, saline subsurface layer is reproduced. Furthermore, the model clearly captures and explains how this saline layer forms from autumn to spring because the formation of sea ice (with residual salinity of ~ 5 psu) injects salt to the ocean surface. This process results in coastal dense water formation^[38]. Sea ice starts forming in October and continues to April, providing salty, cold water to form the saline layer. This phenomenon is one of the important coastal processes revealed by the CIOM. The temperature in transect 2 also shows that cold water formed during the winter seasons in the subsurface layer can survive the summer (not shown).

Figure 5 shows a winter section in the Canadian Beaufort Sea (see section 5 in Fig. 4), as simulated by CIOM. The observations (lower right panel) indicate upwelled^[10], warm Atlantic Water with subsurface, dome-shaped structure. The surface winter water is around the freezing temperature during winter. The model also shows the upwelled Atlantic Water with an upwelled tongue, particularly in the winter.

Figure 6 shows the alongshore velocity to transect 6 (see the inserted panel in Fig. 4 for the location) where velocity measurements were conducted by a high-resolution ADCP array^[3]. The observed subsurface core current or the so-called BSC was captured by the model, consistent with the measurements. The observations show three types of slope current structure. One is the westward at the surface and the eastward slope current at subsur-

face, which is captured from April to July by the CIOM. The second type of structure is the subsurface jet flowing to the east, which is captured by CIOM from January to March. The third type of structure has the surface eastward flow that the CIOM can reproduce from August to December. Note that the CIOM-simulated results are free of data assimilation.

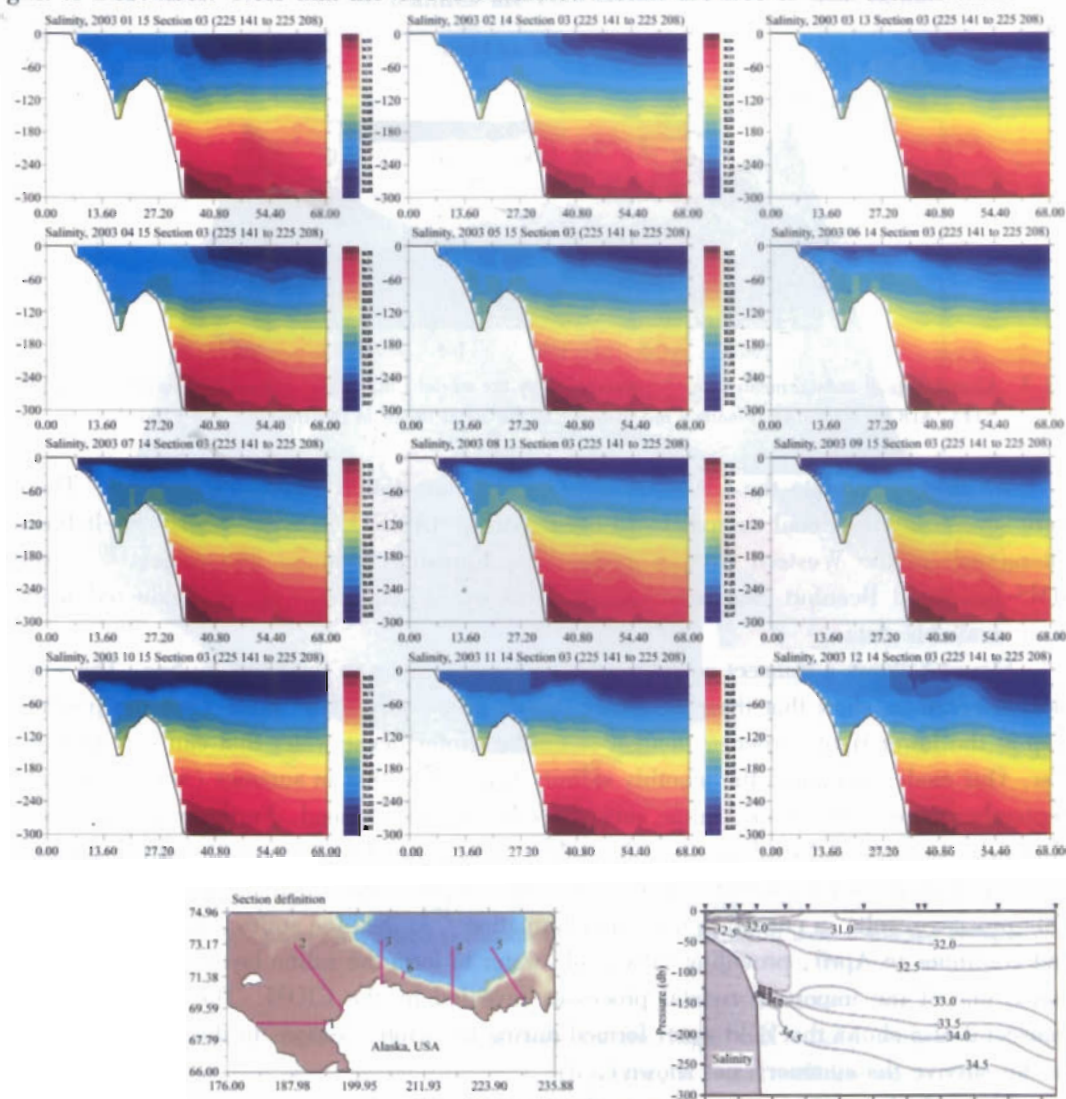


Fig. 4 The CIOM-simulated monthly salinity in transect 3 (see the lower left map) from left to right and top to bottom: Jan., Feb., Mar., Dec., which reveals a thick, saline subsurface layer as observed in the summer survey by Weingartner *et al.* (1998, see the lower right map).

Pacific waters entering the Chukchi Sea enter the Arctic Ocean via three branches: ACW branch, Herald Valley branch and Central Channel branch^[39], as discussed above (see Figs. 1 and 2). The oceanic heat transport via these three branches is the key for sea ice melting. In particular, the overwintering of the Pacific waters could be one of the major reasons for the recent ice reduction in the Western Arctic^[40].

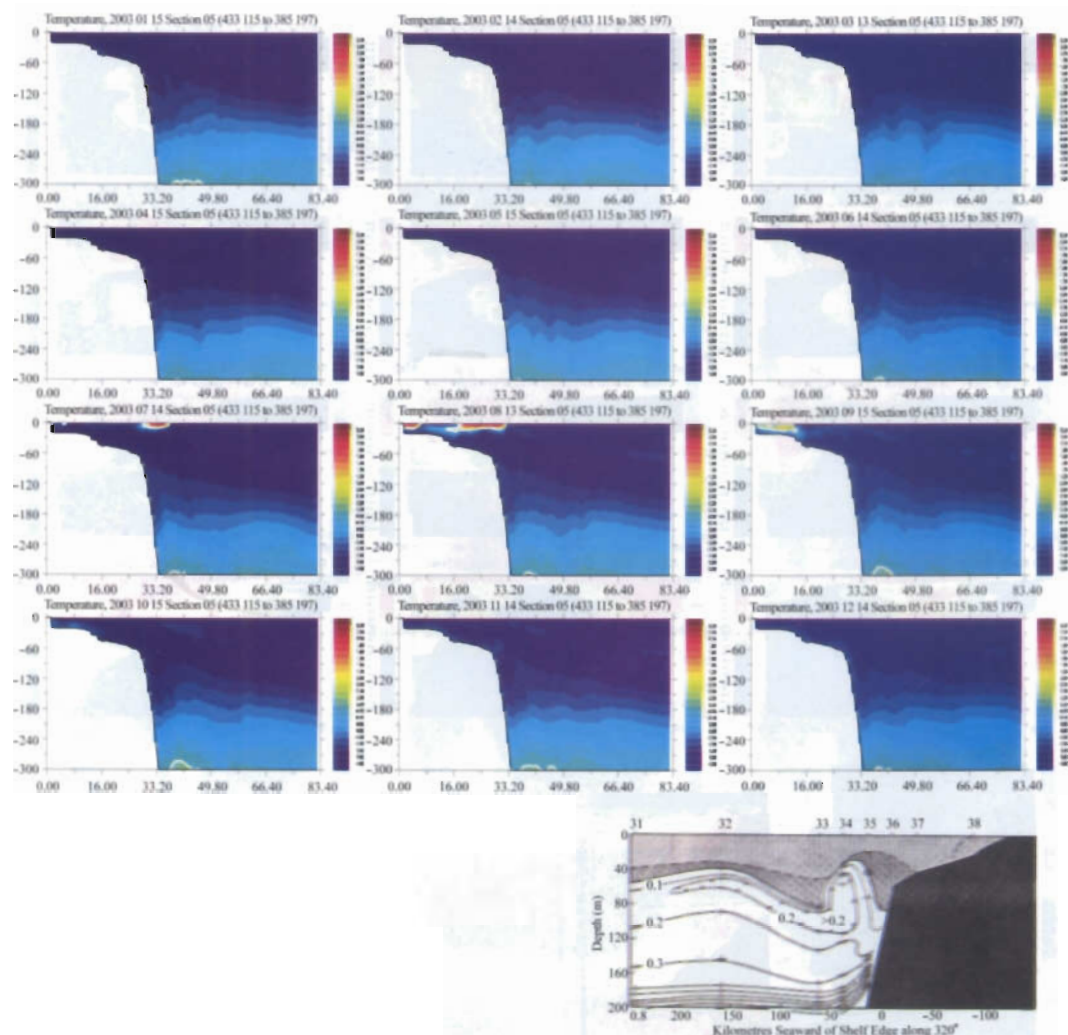


Fig. 5 The CIOM-simulated monthly temperature in transect 5 from left to right and top to bottom: Jan., Feb., Mar., Dec., which reveals a winter upwelling along the Beaufort coast due to the anticyclonic wind forcing. Observations for winter 1990 are shown in lower right corner of the figure^[10].

Figures 7, 8, and 9 show the seasonal variations of temperature, salinity, and northward velocity, respectively, in transect 1. The salinity section (Fig. 7) captures a seasonal freshening in summer and salinization in winter due to saline injection, in particular along the ACW current. The ESC waters are freshest, while the ACW is the second freshest^[41]. We also observed that the bottom waters are saltier because the saltier waters come from the Anadyr Current water and form locally during fall-winter seasons (see October to April), consistent qualitatively with the measurements of Weingartner *et al.* (2005)^[39]. The saltier waters are enhanced in summer, because the Bering inflow consists of the fresher, nutrient-poor ACW and the saltier, nutrient-rich Anadyr Current water. Along with the ESC, this section captures the encountering of these three water masses.

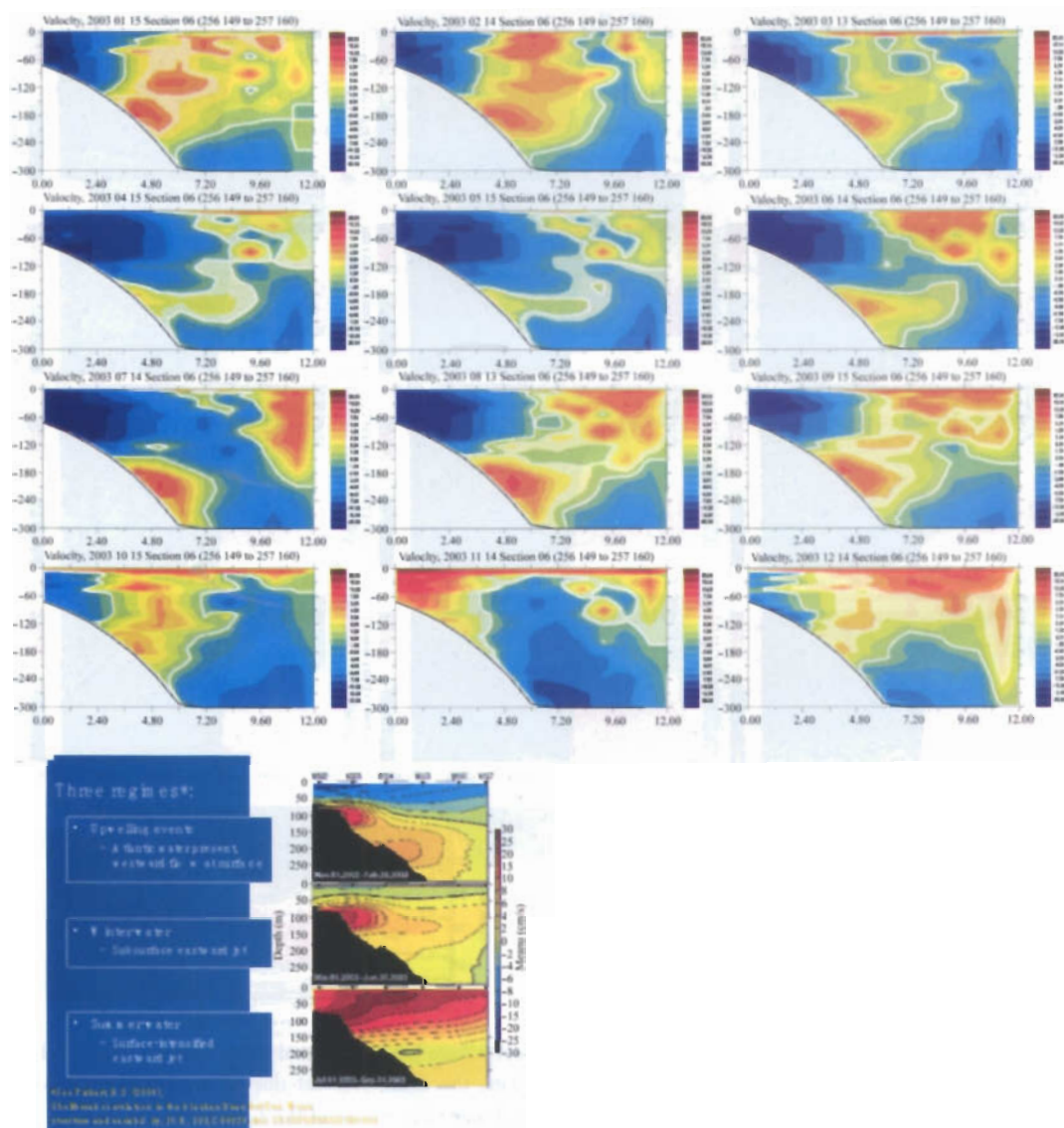


Fig. 6 (Upper) The CIOM-simulated the alongshore current at transect 6 (see the inserted panel in Fig. 6 for the location) from left to right and top to bottom: Jan., Feb., Mar., Dec., which reveals intraseasonal variation of the Beaufort Slope Current (BSC) (Lower) The subsurface core current was observed by a high resolution ADCP array at this transect by Pickart (2004) [3].

The temperature section (Fig. 8) indicates the seasonal cooling-warming variations. The major features simulated include 1) the Bering Inflow advects warm water in summer and cold water in winter into the Chukchi Sea, 2) from fall to winter, the water column is well-mixed due to cooling and tidal stirring, 3) the Pacific waters can survive winter (see maps of Jan. to May), and 4) ESC water is coldest year round. These simulated features coincide qualitatively with the available measurements [39,41].

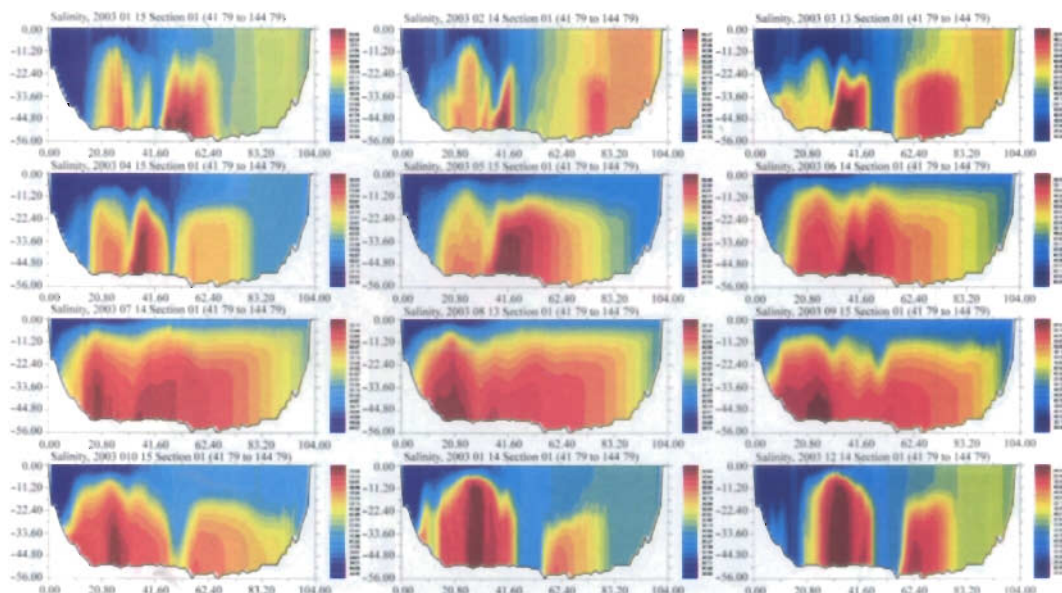


Fig. 7 Same as Fig. 4, except for section 1 salinity.

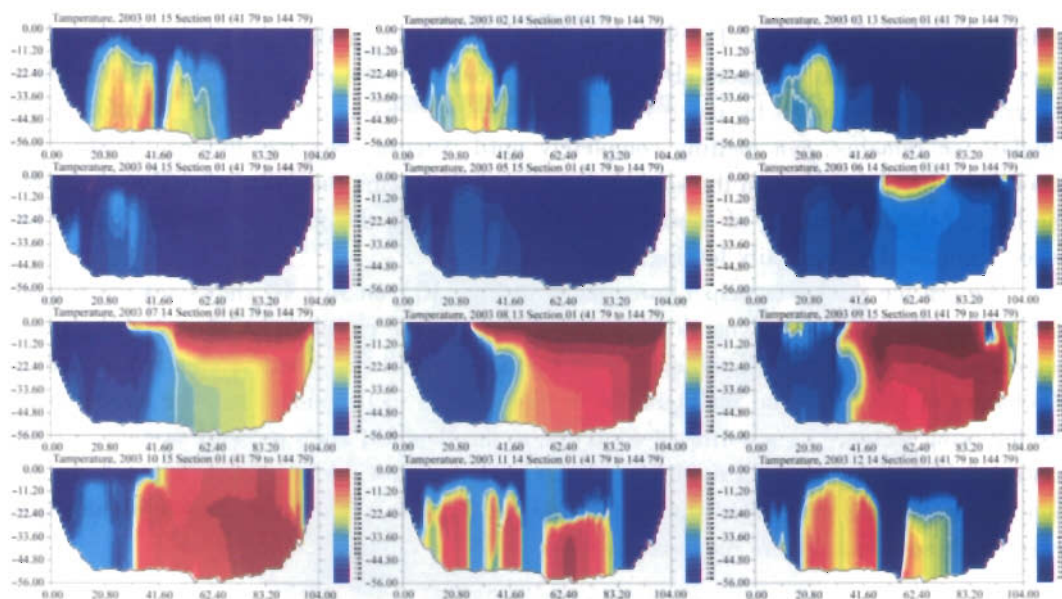


Fig. 8 Same as Fig. 4, except for section 1 temperature.

The velocity section (Fig. 9) shows the Bering inflow is dominant in summer. While the ACW current tends to be barotropic in nature, the ESC appears full of eddies, consistent with the buoyancy-driven characteristics described by Weingartner *et al.* (1999) [41].

3.2 Sea ice ridging and landfast ice

Figure 10 shows sea ice concentration (SIC) and thickness on July 10 under the cli-

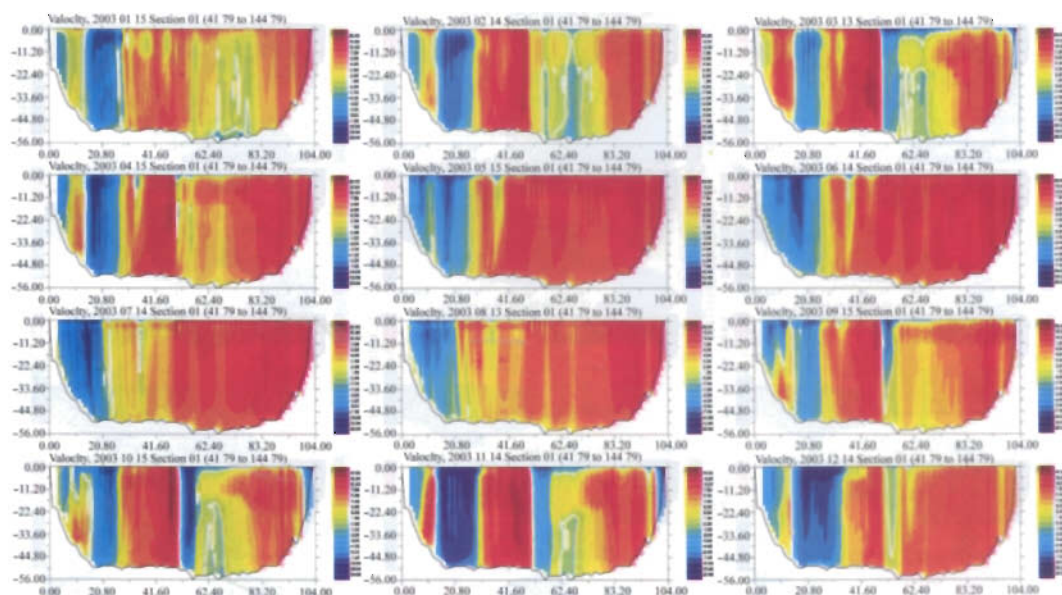


Fig. 9 Same as Fig. 4, except for section 1 velocity; red (blue) denotes northward (southward).

matological monthly forcing. The SIC map (Fig. 10, upper) indicates various shapes of ice floes during the melting season. During spring, sea ice melts offshore first, and the pack ice gradually melts piece by piece into various shapes. Even in July, the Beaufort coast landfast ice remains, not melting completely until August. Sea ice arching, leads, and cracks can be observed from the simulated seasonal SIC maps (not shown). The reason for the late (August) melting of landfast ice may be due to the monthly forcing that is too weak, compared to the daily forcing.

The sea ice thickness map (lower panel of Fig. 10) on July 10 shows sea ice ridging and rafting due to sea ice dynamic interaction with oceanic circulation pattern, shear, convergence, and divergence. Landfast ice along the Beaufort Sea coast is clearly simulated. Mechanics of formation and maintenance of landfast ice in the model may be attributed to the following factors: 1) a northeast wind due to the Beaufort High pressure system, 2) the eastward ACW current has a right-turning force due to the Coriolis effect, 3) high resolution topography and geometry, and 4) internal sea ice stress. However, how to identify and quantify these major factors remains open.

3.3 Comparison of model simulation with satellite measurements

The seasonal cycles of the Beaufort and Chukchi sea ice is well reproduced in comparison to the satellite-measured sea ice area as shown in Fig. 11. Figure 11 indicates the model does not capture the summer minimum sea ice area, although the overall seasonal cycle is well reproduced. Note that the SSM/I does not identify ice ponds (i.e., melting water ponds on the sea ice) from sea water (R. Kwok, personal comm., 8/2006); thus, the satellite observed sea ice area minimum (black line) may underestimate the summer sea ice area (i.e., overestimate the open water). Nevertheless, CIOM still needs to be improved.

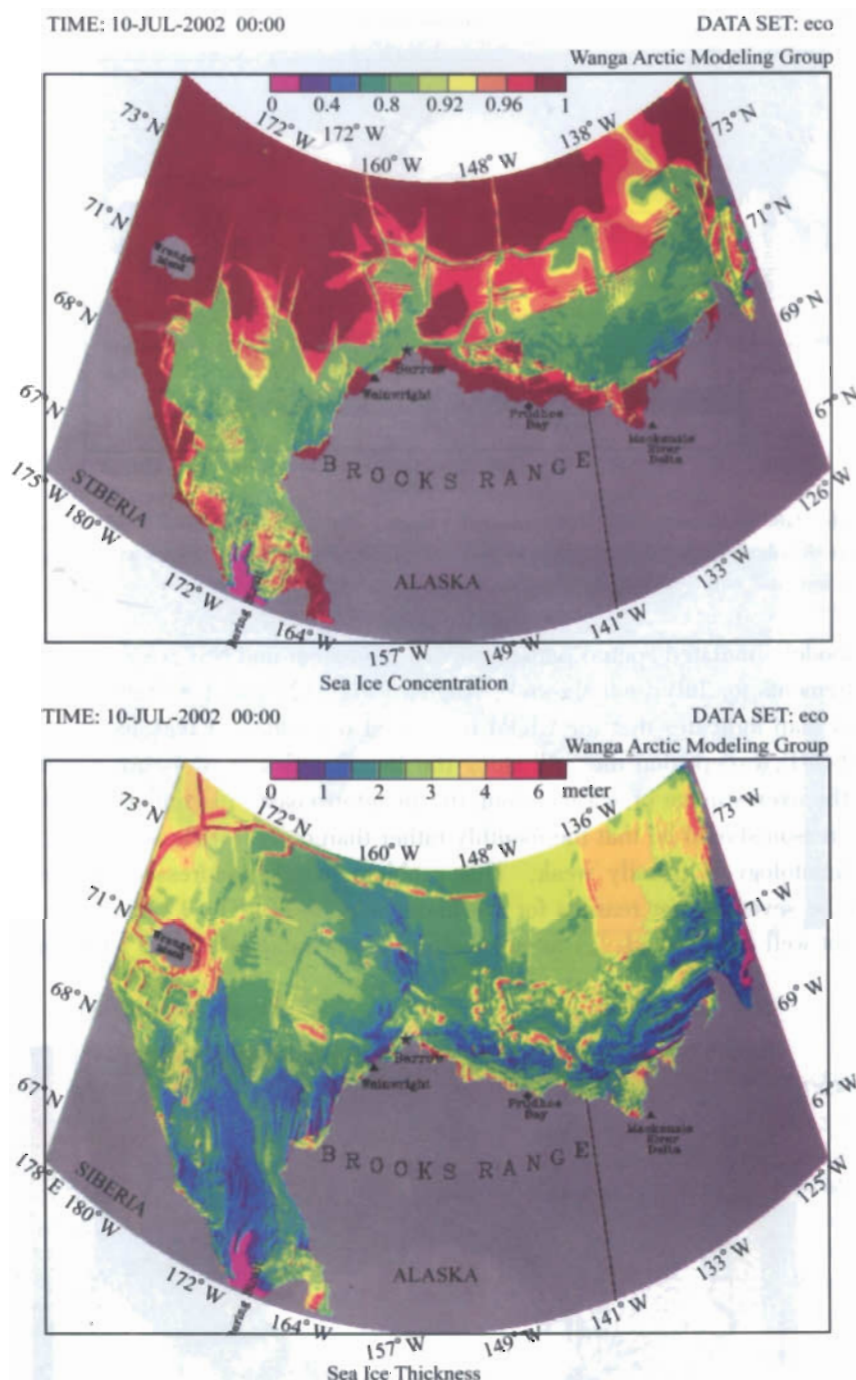


Fig. 10 The sea ice concentration (top; scale: from 0 to 1) and sea ice thickness (bottom panel) on July 10, as simulated by the high-resolution Coupled Ice-Ocean Model (CIOM) [17,22] that is nested to the Japan CCSR/NIES/FRCGC (Center for Climate System Research/National Institute of Environmental Studies/Frontier Research Center for Global Change) high-resolution global model. Sea ice breaks up offshore piece by piece; landfast ice remains untouched along the Beaufort Sea coast. Sea ice floes are irregular in shape and break away from pack ice. Sea ice ridging, rafting, and openings/leads can be well reproduced by sea ice thickness (bottom panel).

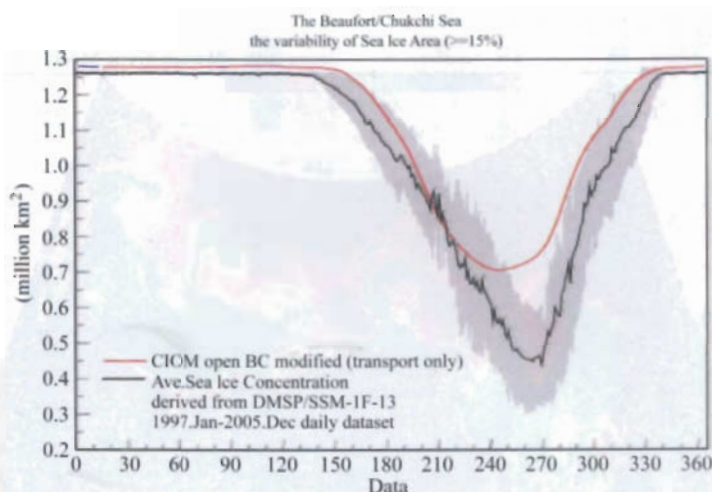
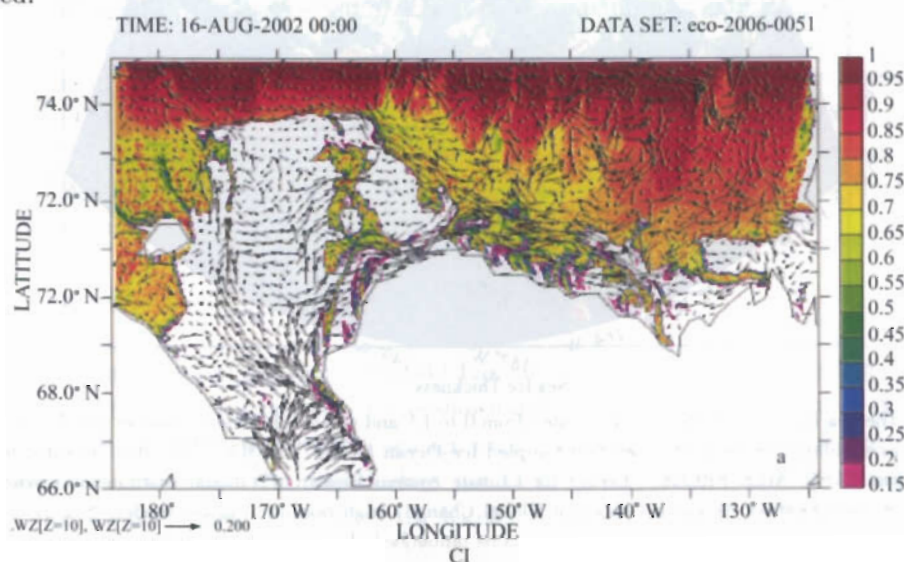


Fig. 11 Model-data comparison; Satellite-measured (black) and model-simulated (red) sea ice cover; For more details of the satellite products prepared for validation of CIOM, please go to: <http://www.frontier.iarc.uaf.edu/~jwang/SatelliteProducts>

The model-simulated spatial patterns of sea ice extent and SST were compared to satellite measurements for July (not shown), August (Fig. 12), and September (not shown). The August map indicates that the CIOM in general reproduces a reasonable spatial pattern of SIC and SST, except that the SST along the Beaufort Sea coast is underestimated. This results in the overestimate of sea ice along the Beaufort coast, particularly the landfast ice. The major reason should be that the monthly rather than daily forcing was used, because the monthly climatology is usually weak. This problem will be addressed in another study. There may be several other reasons for the underestimate of SST: 1) the warm Bering Sea inflow is not well represented, 2) lateral melting is not included, and 3) tidal mixing is not included.



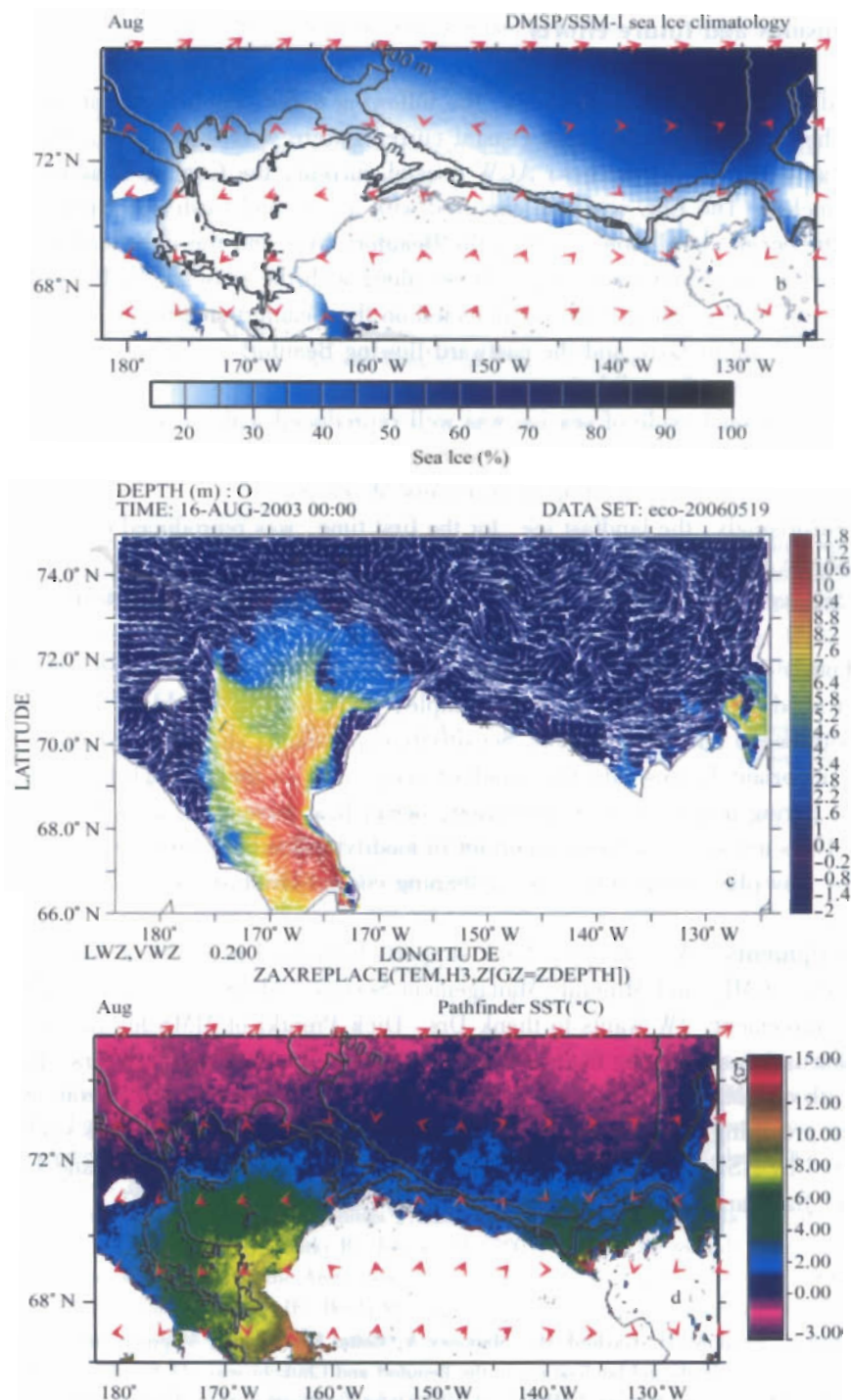


Fig. 12 The comparison between the CIOM-simulated SIC (a) and SST (c) and satellite-measured SIC (b) and SST (d). Superimposed into the modeled SIC and SST maps are the surface ocean currents (a, c), while superimposed into the remote sensed SIC and SST maps are the NCEP wind vectors (b, d).

4 Conclusions and future efforts

Based on the above investigations, the following major conclusions can be drawn:

1) The Chukchi-Beaufort seas coastal currents were well reproduced. The Bering inflow separates into three branches: ACW coastal current, the Central Channel and Herald Valley branches. The ESC was also captured with a cold and fresh water mass.

2) The ocean circulation, such as the Beaufort Gyre and the imbedded mesoscale eddies with anticyclones outnumbering cyclones along with the seasonal cycle, were very well simulated. A deep trough in SSH was detected on the Beaufort shelfbreak between the westward-flowing Beaufort Gyre and the eastward-flowing Beaufort coastal current, which needs further measurements for validation.

3) The seasonal cycle of sea ice was well reproduced with some discrepancy from the satellite measurements. Without lateral melting, the CIOM produces more sea ice along the Beaufort coast in summer, leading to an excess of sea ice.

4) Surprisingly, the landfast ice, for the first time, was reproduced even under monthly atmospheric forcing.

5) Sea ice ridging, cracks, arching, and other downscaling characteristics were captured.

Although many dynamic and thermodynamic features were revealed and discussed, there is a need for future efforts. For example, daily forcing should be very important in driving both ocean and sea ice flow. Sensitivity experiments should be conducted to reveal the most important factors affecting landfast ice, such as daily (high-frequency storms) wind, the Bering inflow, sea ice advection, ocean heat advection, and the lateral melting process. Tides are weak and less important in modifying landfast ice distribution. Nevertheless, tides may play a important role in shaping coastal landfast ice.

Acknowledgments We sincerely thank supports from the University of Alaska Coastal Marine Institute (CMI) and Minerals Management Service (MMS) and IARC/JAMSTEC Cooperative Agreement. JW wants to thank Drs. Dick Prentki of MMS for valuable guidance and for discussion during the course of this research. Thanks also go to Drs. Ron Lai and Caryn Smith of MMS for their inputs. JW also wants to thank Dr. Vera Alexander, CMI director, for providing research vision in the Beaufort and Chukchi seas. This study was partly supported by NSF OPP Project ARC-0712673 awarded to Yanling Yu and Hajo Eicken (PIs) and Jia Wang (co-PI). This is GLERL Contribution No. 1497.

References

- [1] Eicken H; Shapiro LH, Gaylord AG, Mahoney A, Cotter PW(2005): Mapping and characterization of recurring spring leads and landfast ice in the Beaufort and Chukchi seas. U.S. Department of Interior, Minerals Management Service (MMS), Alaska Outer Continental Shelf Region, Anchorage, Alaska, 141.
- [2] Weingartner TJ, Cavalieri DJ, Aagaard K, Sasaki Y(1998): Circulation, dense water formation, and outflow on northeast Chukchi shelf. *J. Geophys. Res.*, 103:7647-7661.
- [3] Pickart RS(2004): Shelfbreak circulation in the Alaska Beaufort Sea: Mean structure and variability. *J. Geophys. Res.*, 109:C04024 doi: 10.1029/2003JC001912.

- [4] Manley TO, Hunkins K(1985) : Mesoscale eddies of the Arctic Ocean. *J. Geophys. Res.* , 90:4911 – 4930.
- [5] Muench RD, Gunn JT, Whitledge TE, Schlosser P, Smethie W(2002) : An Arctic Ocean cold core eddy. *J. Geophys. Res.* , 105 (C10) : 23,997 – 24,006.
- [6] Chao SY, Shaw PT(2002) : A numerical investigation of slanted convection and subsurface anticyclone generation in an Arctic baroclinic current system. *J. Geophys. Res.* , 107(C3) :3019, doi:10.1029/2001JC000786.
- [7] Nihoul JCJ, Adam P, Brasseur P, Deleersnijder E, Djenidi S, Haus J(1993) : Three-dimensional general circulation model of the northern Bering Sea's summer ecohydrodynamics. *Contin. Shelf Res.* , 13: 509 – 542.
- [8] Kowalik Z, Proshutinsky A(1994) : The Arctic Ocean Tides, In: *The Polar Oceans and Their Role in Shaping the Global Environment: Nansen Centennial Volume*. *Geoph. Monograph, AGU*, 85:137 – 158.
- [9] Yang J(2006) : The seasonal variability of the Arctic Ocean Ekman transport and its role in the mixed layer heat and salt fluxes. *J. Clim.* , 19:5366 – 5387.
- [10] Melling H(1993) : The formation of a haline shelf front in wintertime in an ice-covered sea. *Contin. Shelf Res.* , 13:1123 – 1147.
- [11] Mahoney A, Eicken H, Gaylord AG, Shapiro L(2007a) : Alaska landfast sea ice: Links with bathymetry and atmospheric circulation. *J. Geophys. Res.* , 112:C02001, doi:10.1029/2006JC003559.
- [12] Mahoney A, Eicken H, Shapiro L(2007b) : How fast is landfast ice? A study of the attachment and detachment of nearshore ice at Barrow, Alaska. *Cold Regions Science and Technology*, 47:233 – 255.
- [13] Shuert PG, Walsh JJ(1993) : A coupled physical – biological model of the Bering – Chukchi seas. *Contin. Shelf Res.* , 13:543 – 573.
- [14] Grebmeier JM, Overland JE, Moore SE, Farley EV, Carmack EC, Cooper LW, Frey KE, Helle JH, McLaughlin FA, McNutt SL(2006) : A major ecosystem shift in the Northern Bering Sea. *Science*, doi: 10.1126/science.1121365, 311:1461 – 1464.
- [15] Winsor P, Chapman D(2004) : Pathways of Pacific water across the Chukchi Sea: A numerical model study. *J. Geophys. Res.* 109, C03002, doi:10.1029/2003JC001962.
- [16] Yao T, Tang CL, Peterson IK(2000) : Modeling the seasonal variation of sea ice in the Labrador Sea with a coupled multi-category ice model and the Princeton. *Ocean Model.* , *J. Geophys. Res.* , 105 (C1) :1153 – 1165.
- [17] Wang J, Liu Q, Jin M(2002a) : A User's Guide for a Coupled Ice-Ocean Model (CIOM) in the Pan-Arctic and North Atlantic Oceans. *International Arctic Research Center-Frontier Research System for Global Change, Tech. Rep.* 02 – 01, 65.
- [18] Wang J, Liu Q, Jin M(2002b) : A nested coupled ice-ocean model for the Beaufort Sea. *Annual Report No. 8*, University of Alaska, MMS/Alaska OCS Region, Anchorage, Dept. of the Interior, 80 – 94.
- [19] Wang J, Jin M, Ikeda M, Shimada K, Takahashi J(2003a) : Validation of a nested coupled ice-ocean model in the Beaufort Sea. *Annual Report No. 9*, University of Alaska, MMS/Alaska OCS Region, Anchorage, Dept. of the Interior, 19 – 31.
- [20] Wang J, Kwok R, Saucier FJ, Hutchings J, Ikeda M, Hibler WIII, Haapala J, Coon MD, Meier HEM, Eicken H, Tanaka N, Prentki R, Johnson W(2003b) : Working towards improved small-scale sea ice and ocean modeling in the Arctic seas. *EOS, AGU*, 84(34) : 325, 329 – 330.
- [21] Wang J, Wu B, Tang C, Walsh JE, Ikeda M(2004) : Seesaw structure of subsurface temperature anomalies between the Barents Sea and the Labrador Sea. *Geophys. Res. Lett.* , 31:L19301, doi: 10.1029/2004GL019981.
- [22] Wang J, Liu Q, Jin M, Ikeda M, Saucier FJ(2005) : A coupled ice-ocean model in the pan-Arctic and the northern North Atlantic Ocean; Simulation of seasonal cycles. *J. Oceanogr.* , 61:213 – 233.
- [23] Mellor GL(2004) : Users guide for a 3-D, primitive equation, numerical ocean model. *Atmospheric and Oceanic Sciences Program, Princeton Univ. (Princeton, NJ 08540)*, 39.
- [24] Hibler WD III(1980) : Modeling a variable thickness sea ice cover. *Mon. Wea. Rev.* , 108:1943 – 1973.

- [25] Hu HG, Wang J(2008): Modeling the ocean circulation in the Bering Sea. *Ocean Modeling* (this volume).
- [26] Wang J, Hu HG, Mizobata K, Saitoh S(2009): Seasonal variations of sea ice and ocean circulation in the Bering Sea: A model-data fusion study. *J. Geophys. Res.*(in press).
- [27] Wang J, Jin M, Ikeda M, Shimada K, Takahashi J(2003c): The validation of a nested coupled ice-ocean model in the Beaufort Sea. Annual Report No. 9, University of Alaska, MMS/Alaska OCS Region, Anchorage, Dept. of the Interior.
- [28] Wang J, Jin M, Patrick V, Allen J, Eslinger E, Mooers C, Cooney T(2001): Numerical simulation of the seasonal ocean circulation patterns and thermohaline structure of Prince William Sound, Alaska. *Fisheries Oceanogr.*, 10 (Suppl. 1), 132 – 148.
- [29] Wang J, Patrick V, Allen J, Vaughan S, Mooers CNK, Jin M(1999): Modeling seasonal ocean circulation of Prince William Sound, Alaska using freshwater of a line source. In *Coastal Engineering and Marina Development*, eds. CA Brebbia and P Anagnostopoulos. WIT Press, Southampton-Boston, 55 – 66.
- [30] Hibler WD III(1979): A dynamic and thermodynamic sea ice model. *J. Phys., Oceanogr.*, 9;5,959 – 15,969.
- [31] Wang J, Mysak LA, Ingram RG(1994): A numerical simulation of sea-ice cover in Hudson Bay. *J. Phys. Oceanogr.*, 24: 2515 – 253.
- [32] Thorndike AS, Rothrock DA, Maykut GA, Colony R(1975): The thickness distribution of sea ice. *J. Geophys. Res.*, 80: 4,501 – 4,513.
- [33] Mellor GL, Kantha L(1989): An ice-ocean coupled model. *J. Geophys. Res.*, 94: 10,937 – 10,954.
- [34] kantha LH, Clayson CA(1994): An improved mixed layer model for the Antarctic ice melt season. *J. Phys. Oceanogr.*, 35:188 – 201.
- [35] Steele M, Rebecca R, Ermold W(2001): PHC: A global ocean hydrography with a high – quality Arctic Ocean. *J. Climate*, 14:2079 – 2087.
- [36] Woodgate R, Weingartner TJ, Aagaard K(2005): A year in the physical oceanography of the Chukchi Sea: Moored measurements from autumn 1990 – 1991. *Deep Sea Res. II*, 3116 – 3149.
- [37] Wang J, Ikeda M(1997): Diagnosing ocean unstable baroclinic waves and Meanders using quasi-geostrophic equations and Q-vector method. *J. Phys. Oceanogr.*, 27(6): 1158 – 1172.
- [38] Wang J, Ikeda M, Saucier F(2003d): A theoretical, two-layer, reduced-gravity model for descending dense water flow on continental slopes. *J. Geophys. Res.*, 108 (C5): 3161, doi: 10.1029/2000JC000517.
- [39] Weingartner TJ, Aagaard K, Woodgate R, Danielson S, Sasaki Y, Cavalieri DJ(2005): Circulation on the north central Chukchi Sea shelf. *Deep Sea Res. II*, 3150 – 3174.
- [40] Shimada K, Kamoshida T, Itoh M, Nishino S, Carmack E, McLaughlin F, Zimmermann S, Proshutinsky A(2006): Pacific Ocean inflow: Influence on catastrophic reduction of sea ice cover in the Arctic Ocean. *Geophys. Res. Lett.*, 33:L08605, doi:10.1029/2005GL025624.
- [41] Weingartner TJ, Danielson S, Sasaki Y, Pavlov V, Kulakov M(1999): The Siberian Coastal Current: a wind and buoyancy-forced arctic coastal current. *J. Geophys. Res.*, 104: 29,697 – 29,713.

